

# SEISMIC EVENT LOCALIZATION IN AN ANISOTROPIC ENVIRONMENT

*D. Gajewski, K. Sommer, C. Vanelle, and R. Patzig*

**email:** *dirk.gajewski@zmaw.de*

**keywords:** *Localization, Anisotropy*

## ABSTRACT

*The environment of the German Continental Deep drilling site (KTB) is known to be anisotropic. In this study, we have analyzed seismic events generated by the KTB long term injection experiment. More than 2500 seismic events were generated. About 260 events were recorded by the borehole geophone and by the 42 station surface array centered at the KTB. For this experiment, we are in the favorable position to have a priori knowledge where the acoustic emissions should originate, i.e., they should start at the injection point and slowly propagate away from it. Localizing the events with a homogeneous isotropic model based on average velocities derived from check shots leads to a lateral southward shift of the center of the event cloud of about 500m away from the injection point. Since the total extension of the elongated event cluster is about 2 km in E-W direction and about 300-400 m in N-S direction this is a significant contribution. Using the 3-D heterogeneous isotropic velocity model obtained from the KTB reflection data, no significant change in the localization is observed and the lateral shift is reproduced. Localizing the same events with a homogeneous anisotropic model based on published data from core samples centers the event cloud around the injection point. The anisotropic localization removes the lateral shift of the events. For this data it appears that anisotropy has a much stronger influence on the localization than heterogeneity. Localizing the events with the anisotropic model also significantly alters the shape of the event cloud from an elongated cluster to an almost circular distribution. This is important if the spatio-temporal evolution is interpreted with respect to the hydraulic properties of the rocks. Also, interpretations with respect to event clustering due to tectonics or hydro-fracking may be severely affected if anisotropy is neglected.*

## INTRODUCTION

The problem of earthquake location is one of the most basic problems in seismology. Although numerous applications exist worldwide, the inherent non-linearity in the inversion process prevents earthquake location from being a standardized routine tool. The general strategy of most applications is the minimization of traveltimes differences between observed and predicted events for a considered velocity model. Source location methods can be categorized into absolute location methods and relative location methods. For the first type, the determination of the excitation time and hypocenter of a seismic source is traditionally performed by minimizing the difference between the observed and predicted arrival times of some seismic phases. For recent advances in seismic event location using such approaches see, e.g., Thurber and Rabinowitz (2000). The second class of methods considers relative location within a cluster of events using traveltimes differences between pairs of events or stations, see, e.g., Waldhauser and Ellsworth (2000).

Currently, most of these methods have in common that an isotropic subsurface model is assumed. It is, however, known from seismological studies and reflection seismology that the earth is not isotropic. Not surprisingly, the anisotropy affects the localization of seismicity. In this study, we quantify this effect for the hydraulically-induced seismic events of the KTB injection experiment. A fluid injection experiment provides perfect conditions for a real data case study since a priori knowledge on the event location is

available. The events should start close to the injection point and propagate away from it with increasing injection time. The subsurface of the KTB is known to be anisotropic (Rabbel, 1994; Rabbel et al., 2004) and, therefore, provides an ideal environment for this study.

We used a localization technique based on a grid search approach. It allows to consider 3D-heterogeneous isotropic and anisotropic models. The actual search procedure is the same for both cases except that the tool to generate the traveltimes of the considered events need to be chosen according to the model. The method was verified with synthetic data and then applied to the KTB data for this study. It shows that the neglect of anisotropy can lead to serious mis-localizations and thus to mis-interpretation of the located events. We will first describe the KTB injection experiment before we briefly explain the localization method. After this, we discuss the anisotropy of the KTB and present of localization results for the induced seismicity using isotropic and anisotropic subsurface models. Discussions and conclusions finalize the paper.

## EXPERIMENT

The continental deep drilling site (KTB) is located at the western margin of the Bohemian Massif, a large exposed complex within the Variscan Belt of central Europe. The Franconian lineament (FL in Figure 1) cuts through the area of investigation and separates the metamorphic basement in the East from the Permo-Mesozoic cover in the West. The KTB itself is entirely located in a hard rock environment composed of metamorphic rocks (mostly gneiss). During the KTB injection experiment performed in the year 2000, a total of more than 4000 m<sup>3</sup> of water were injected into the KTB over a period of 60 days. The entire borehole was pressurized. The purpose was to generate micro-seismicity around the open-hole section at a depth of about 9 km to investigate the hydraulic properties. More than 2500 seismic events were generated (Baisch et al., 2002). The events were observed by a surface network, which consisted of 42 stations, including a borehole geophone which was placed in the pilot hole located 200 m to the west of the KTB at a depth of about 4 km (Figure 1). The borehole geophone was recording at 1000 Hz sampling frequency, while the surface network operated at 200 Hz. Due to a leakage of the casing near 5 km in depth about 75 % of the water escaped at this level.

Using the Geiger method (Geiger, 1910), 237 events were localized by Baisch et al. (2002) assuming a homogeneous isotropic velocity model with mean velocities obtained from check shot data. Most of the events published in that work were located to the south of the injection (see Figure 2). The events in 8 – 9 km depth are all east of the borehole. Station corrections were applied in the work of Baisch et al. (2002) and the borehole recordings of the events was assigned a higher weight than the surface observations during their localization procedure. P- and S-arrivals were picked by these authors. No special analysis for shear wave splitting was performed. The same picks are also used in this study. In the next section we will describe the localization technique used.

## LOCALIZATION TECHNIQUE

Almost all localization techniques currently used are minimizing an objective function based on the traveltime differences of observed and predicted onset times of seismic events where an isotropic, and often homogeneous subsurface model is assumed. In the approach used here, we minimize the residual square sum of the measured and the calculated traveltimes determined for different points within the discretized velocity model. The residual square sum provides a measure for the probability that the hypocenter is located at the particular point in the model under consideration. The residual square sum  $R$  is defined as the square of the difference between measured and calculated P- and/or S-traveltimes at each station divided by the inaccuracy of the particular pick:

$$R = \sum_{m=1}^M \left( \frac{t^{(P)} - T^{(P)}}{\Delta t^{(P)}} \right)^2 + \left( \frac{t^{(S)} - T^{(S)}}{\Delta t^{(S)}} \right)^2, \quad (1)$$

where  $T^{(P)}$  and  $T^{(S)}$  are the computed P- and S onset times for the particular subsurface point. The traveltimes  $t^{(P)}$  and  $t^{(S)}$  are the measured P- and S-onset times,  $m$  is the station number with  $m = 1, 2, \dots, M$ , and  $M$  is the number of stations in the recording array on which the event was observed. The picking errors are specified by  $\Delta t^{(P)}$  and  $\Delta t^{(S)}$ . The traveltimes  $T^{(P)}$  and  $T^{(S)}$  are computed using the velocity model under consideration which may be 3-D isotropic or anisotropic. For the case of anisotropic media only the

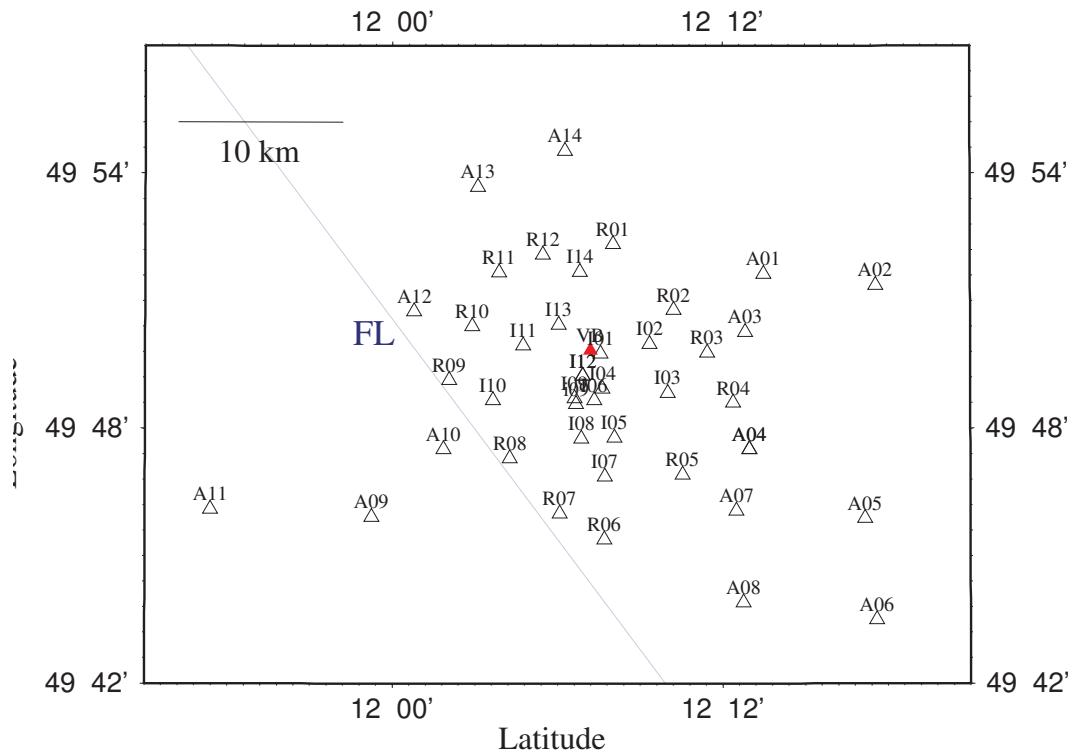


**Figure 1:** The arrangement of the surface network. The projection of the borehole geophone at the surface is marked by the red triangle. The blue line represents the Franconian Lineament as mapped at the surface.

fasted predicted traveltimes of the S-events were considered. The data were not analyzed for shear wave splitting.

According to the residual square sum given in equation 1, the localization of the hypocenter depends not only on the measured onset times, but also on the inaccuracies of the picks. Most localization methods apply weight categories, e.g., from 1 to 4 as described below, depending on the quality of the particular pick. We used the picks and weights as determined by Baisch et al. (2002) after converting their weights into picking errors according to Table 1.

Weight 1 corresponds to a picking error of one sample. This value is 0.005 s for a station of the surface

weight	picking error [s]
1	0.005
2	0.010
3	0.025
4	0.050

**Table 1:** Conversion of weights into picking errors in ms.

network and 0.001 s for the borehole geophone. Because of the higher signal to noise ratio of the borehole geophone its pick inaccuracy is always chosen as one sample. The maximum spacing of the subsurface grid should reflect the prevailing wavelength of the data. Model dimensions and computational limitations may require larger grid spacings. For model grids with spacings noticeably larger than the average wavelength locations between the grid nodes need to be considered. For these locations, traveltimes interpolation techniques are required that take the wavefront curvature into account to achieve higher accuracy, like the

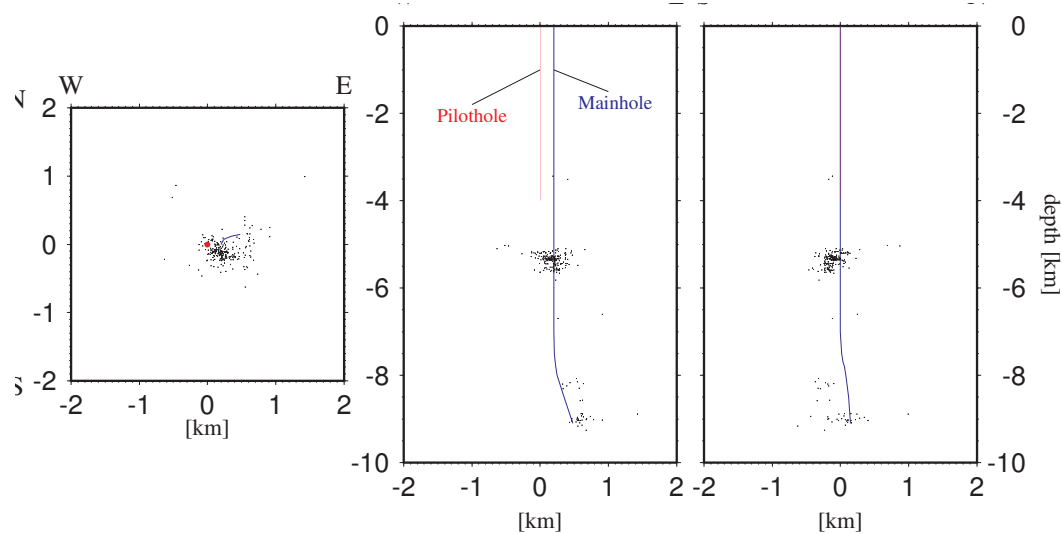


**Figure 2:** Localization of the events of the fluid injection experiment 2000 at the KTB as obtained by Baisch et al. (2002).

hyperbolic interpolation technique of (Vanelle and Gajewski, 2002). Due to of the model dimensions of the KTB data the grid spacing of the subsurface model was as large as to 400 m.

The theoretical traveltimes is computed for every grid point of the discretized subsurface model. For the computation of traveltimes on a 3-D heterogeneous isotropic and anisotropic grid various methods have been established, like FD eikonal solvers (Vidale, 1988, 1990; Ettrich and Gajewski, 1998; Soukina et al., 2003), ray tracing methods (Vinje et al., 1996a,b; Ettrich and Gajewski, 1996; Coman and Gajewski, 2004; Kaschwich and Gajewski, 2003), shortest path (Moser, 1991), or bending techniques. See, e.g., Leidenfrost et al. (1999) for an overview of these techniques and their efficiencies. Quite often homogeneous models are still in use for event localization where analytical solutions can be applied.

After the traveltimes were generated, the node with the lowest residual square sum is considered as the hypocenter of the event under investigation. This minimum of the residual square sum is identified with a grid search algorithm. For this technique, the values of the residual square sum at 27 points of a cube of the subsurface grid are evaluated during each step of the grid search procedure. If the central point shows

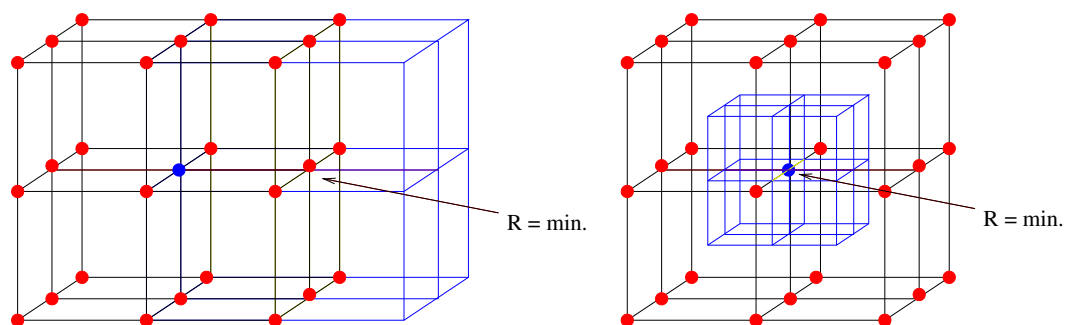


**Figure 3:** For the grid search procedure the residual square sums at 27 points of a cube of the subsurface grid are evaluated. If the central point of the cube shows the lowest value, the cube is reduced to half its size (left). If one of the other points has the lowest value the cube is shifted so that this point now becomes the center of a new cube (right).

the lowest value, the cube shrinks to half of its size, retaining its center, see Figure 3 right. If one of the

surrounding points displays the lowest value, the cube is shifted such that this point becomes the center of the next cube to be investigated (Figure 3 left). This procedure is continued until the size of the cube is below one characteristic wavelength, which corresponds to the maximum spatial resolution that can be achieved for event localization. The residual square sum at the minimum found in the way described above is a measure for the quality of the used model.

The technique can be used for homogeneous and heterogeneous, isotropic or anisotropic media. The grid search and traveltime interpolation are independent of the type of the model (i.e., 1-D, 2-D, 3-D isotropic or anisotropic), only the technique to compute traveltimes on the discretized subsurface grid needs to be adapted to the model under consideration. Therefore, the grid search approach provides a versatile procedure for event localization as it may be applied to different kinds of subsurface models without modification of the search itself. Since anisotropic models are the key issue of this paper we will review the anisotropy of the KTB environment in the following section.

### SEISMIC ANISOTROPY AT THE KTB

After the pilot hole was completed at the KTB site, a number of experiments were performed to determine the seismic anisotropy. The main results of these experiments were (Rabbel, 1994; Rabbel et al., 2004):

- The gneiss in the upper 3.5 km is anisotropic. The polarization direction of the faster shear wave coincides with the NW-SE-strike of the steeply-dipping rock foliation.
- In the depth interval from 2.2 - 3 km the anisotropy can be approximated by a hexagonal symmetry with a non vertical symmetry axis. It is mainly caused by the foliation of the gneiss, leading to an average anisotropy of 2.5 %, 14 % and 5 % for the P-, S1- and S2-wave, respectively.
- Zones of increased anisotropy correlate with zones of increased fracture density.
- The total anisotropy can be divided into two major components:
  - the intrinsic background anisotropy, related to mineral composition and foliation of gneiss,
  - the anisotropy caused by oriented fractures.
- Generally, the KTB rocks displays azimuthal anisotropy that is most often approximated by hexagonal symmetry with a non vertical symmetry axis.

Further information was obtained from the interpretation of VSP data collected during the years 1999 and 2000. These experiments focused on the deeper part of the KTB (Rabbel et al., 2004).

The upper and deeper parts consist mainly of gneiss and show lower P-wave velocities (5.4 – 6.3 km/s) compared to the middle part that is dominated by amphibolite (6.3 – 6.8 km/s). Average S-wave velocities are 3.5 – 4.0 km/s and 3.3 – 3.6 km/s, respectively, for the gneiss and 3.6 – 4.0 km/s and 3.5 – 3.9 km/s, respectively, for the amphibolite. The main properties of the three observed depth levels are summarized as follows (Rabbel et al., 2004):

- 2.2 – 3 km: the anisotropy of P-, S1- and S2-waves is 4.4 %, 9.0 % and 3.5 %, respectively. The average isotropic P- and S- wave velocities are 6.12 km/s and 3.15 km/s, respectively.
- Middle section: the material is the same as in the shallower level. It shows 3.9 % lower average P-wave velocity (5.88 km/s) and 0.8 % lower average S-wave velocity (3.48 km/s), whereas the anisotropy increases (6.1 %, 11.7 % and 6.2 %, respectively).
- 7.9 – 8.2 km: a further decrease of the velocities and increase of anisotropy was found, namely 13.2 %, 18.3 % and 3.8 % for maximum estimates of the anisotropy of the P-, S1-, and S2-waves, respectively. The average isotropic velocities are 5.67 km/s and 3.37 km/s, respectively, for P- and S-waves.

While the velocity decreases in the deeper part of the KTB the anisotropy increases at that depth. The anisotropy of the KTB environment is of orthorhombic or lower symmetry, but is usually approximated by a medium of hexagonal symmetry (Jahns et al., 1994a). The symmetry axis varies with depth where its orientation is tied to the geological structure, i.e. the symmetry axis is perpendicular to the foliation of the gneiss. The orientation of this foliation changes considerably with depth. Obviously, the anisotropy at the KTB is rather complicated and of significant magnitude. It affects the localization of seismic events which is shown in the next section.

## RESULTS

Despite the complexity of the KTB environment isotropic homogeneous models derived from check shot data were used so far for the localization of events (Baisch et al., 2002). With this model ( $v_P=6080$  m/s and  $v_S=3510$  m/s) we obtained the localizations shown in Figure 4. The center of the event cloud is shifted

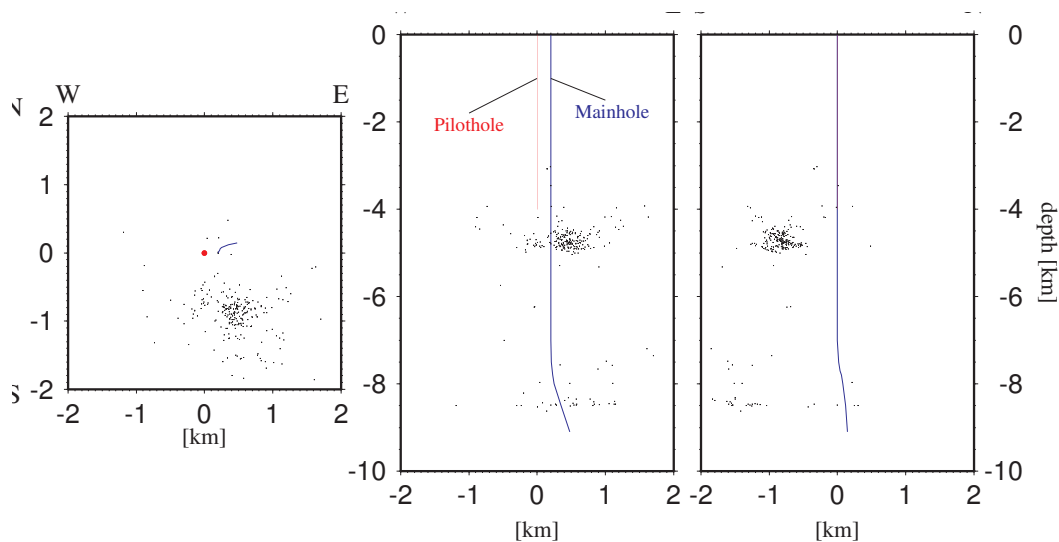


**Figure 4:** Localization with a homogeneous model ( $v_P=6080$  m/s and  $v_S=3510$  m/s). The center of the event cloud is shifted to the south of the injection point by about 500 m.

to the south w.r.t. the injection point by about 500 m, corresponding to 25 % of the total extent of the event cloud. This is a physically unreasonable distribution of events since the center of the event cloud is not centered at the injection point but set off to the south. The localization of Baisch et al. (2002) shown in Figure 2 could not be reproduced, since we did not apply station corrections. Station corrections are applied in seismology if local site effects are present below certain stations of the network, e.g., due to a changing geology below the array, similar to static corrections in the presence of topography. We think that station corrections are inappropriate for the KTB data, since almost all stations are located on the same geological strata. Only for the three receivers to the west of the Franconian Lineament (Figure 1) station corrections might be appropriate since they are located on the Permo-Mesozoic cover. The effect, however, should be rather small, since only a very short segment of the total ray path is affected due to the small thickness of the sediments below these stations. In addition to the station corrections, Baisch et al. (2002) also applied station weights in the localization process to emphasize the borehole geophone 10 times stronger for P-wave events and 7 times stronger for S-wave events compared to the surface stations. Overweighting the shorter raypaths of the borehole receiver reduces the dependence of the localizations on anisotropy since these effects are more pronounced for longer ray paths.

Using a 3D heterogeneous isotropic velocity model derived from the 3-D KTB reflection data (Buske, 1999), no significant changes in the localization were observed (not shown here). The lateral shift of the event cloud is still present with this heterogeneous model. We have also applied other localization tools to

the data like SimulPS (Evans et al., 1994) which is based on the well known Geiger method (Geiger, 1910). This localization method and the homogeneous isotropic model lead to an even stronger lateral shift to the south of the center of the event cloud than observed in Figure 2 (not shown here). To estimate the influence

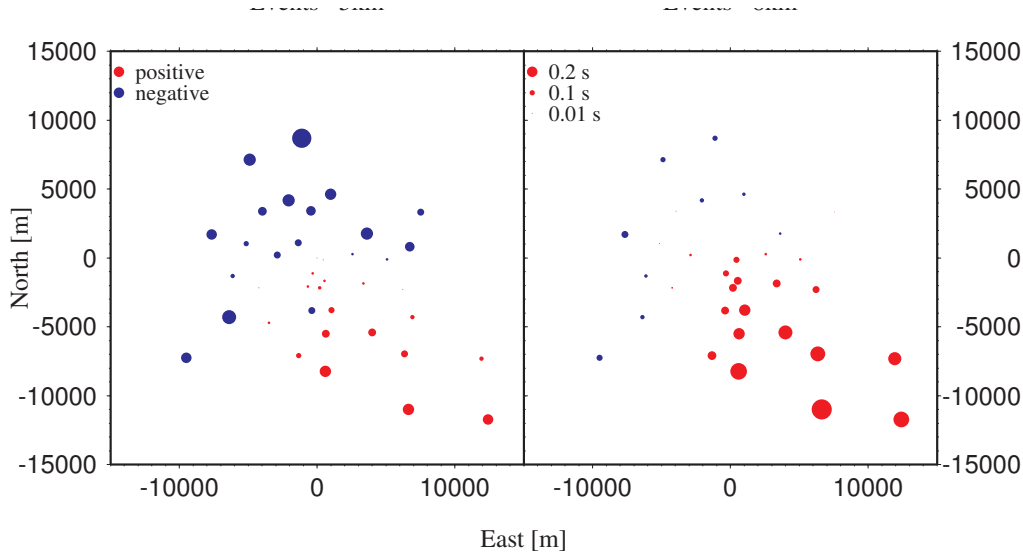


**Figure 5:** Differences of the onset times from the borehole to every station assuming the isotropic homogeneous velocity model and measured onset times. A systematic distribution of differences is obtained.

of station corrections and station weights we determine the deviations between our isotropic homogeneous localization and the isotropic localizations of Baisch et al. (2002). We computed theoretical onset times for each localization and every station assuming the event originated directly at the borehole at 5 km or 8 km depth. The homogeneous isotropic velocity model was used and the traveltimes were compared with the measured onset times. We found a systematical distribution of these differences (Figure 5) which indicates a directional dependence, i.e., anisotropy.

Despite the 3-D complexity of the anisotropy at the KTB we have considered a homogeneous anisotropic model derived from laboratory data. As for the isotropic check shot model this model does not include the 3-D complexity of the study area. For the comparison with the isotropic localization results similar errors with respect to the heterogeneity can be expected. Our anisotropic model is based on elastic parameters determined for KTB rock samples by Jahns et al. (1994b):

$$\underline{A} = \begin{pmatrix} 43.48 & 11.09 & 13.20 & 0.00 & -0.10 & 0.52 \\ & 41.27 & 14.93 & 0.11 & -0.00 & 0.33 \\ & & 33.28 & 0.39 & -0.96 & 0.00 \\ & & & 10.70 & 0.44 & -0.13 \\ & & & & 10.42 & 0.07 \\ & & & & & 15.65 \end{pmatrix} \text{ km}^2/\text{s}^2 \quad (2)$$

The density normalized elastic parameters correspond to a symmetry lower than orthorhombic. The magnitude of the P-wave anisotropy is more than 10%. For the S-waves it is even stronger. The elastic tensor is given in its intrinsic coordinate system and had, therefore, to be rotated with respect to the geological setting and acquisition at the KTB (Figure 6). The rotation was performed in a way that the fastest P-wave velocity of the anisotropic model is aligned along the foliation of the gneiss and the slowest one perpendicular to it as it was determined from the lab measurements of the rock sample.

Despite the homogeneity of this anisotropic model the localization of the data leads to a physically reasonable distribution of events (Figure 7), i.e., the event cloud is almost centered at the injection well. No station corrections or weights were applied here. We observe from the comparison of the isotropic and

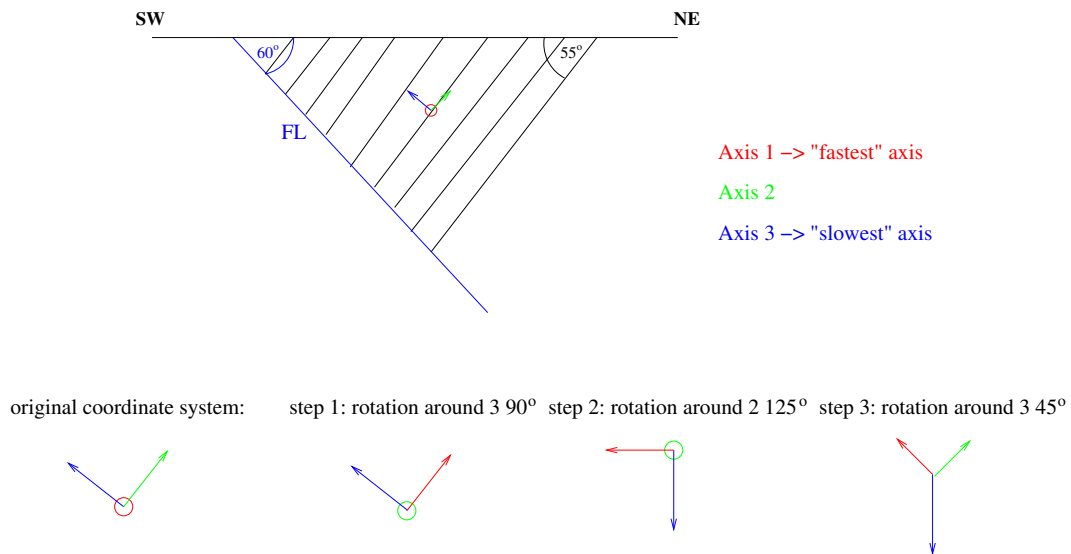


**Figure 6:** Rotation of the elastic tensor to fit the geologic setting (see text). The KTB environment is characterized by steeply-dipping layers of gneiss with a pronounced foliation in the direction of the layering.

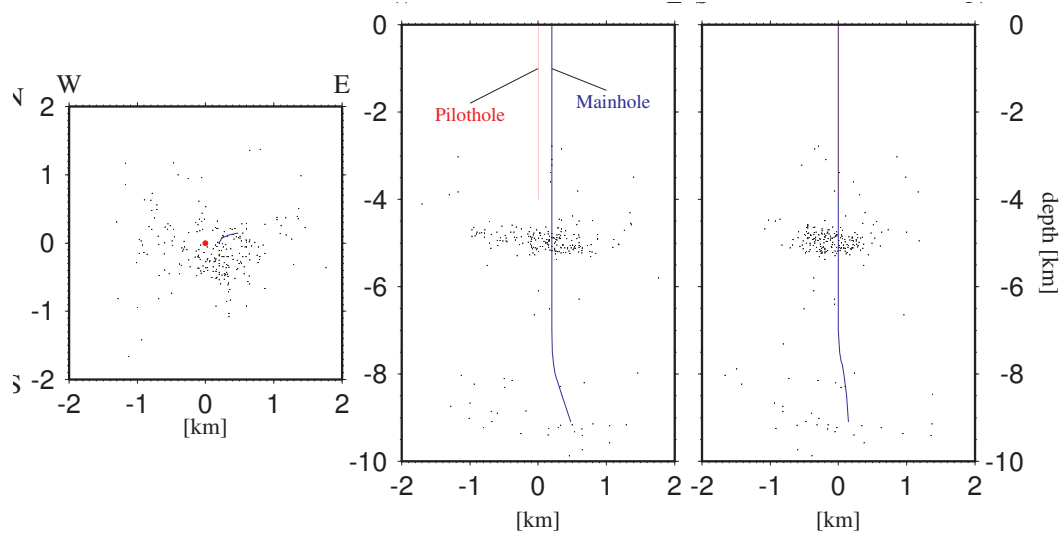


**Figure 7:** Localization with the homogeneous anisotropic velocity model. The cloud of events is centered around the borehole. The lateral shift of events observed for the isotropic model (Figure 4) is not present. The shape of the cloud is now almost circular compared to the elongated shape obtained for the isotropic case (Figure 4).

anisotropic localization that not only the location of the events, but also the shape of the event cloud has changed considerably.

### DISCUSSION AND CONCLUSIONS

The localization of the hydraulically induced seismicity of the KTB injection experiment using an isotropic homogeneous or a 3-D heterogeneous isotropic model shows a strong lateral offset of the center of the event cloud to the south of the injection point. This is a physically unintuitive and unexpected result. To locate the center of the event cloud at about the injection point, the localization with isotropic models requires overweighting of the borehole geophone and station corrections. From several studies of the KTB, its subsurface is known to be anisotropic. Magnitudes of more than 10% velocity anisotropy were reported. Our attempt to use an anisotropic model led to a physically intuitive distribution of events, i.e., the center of the event cloud is located at the injection point. The anisotropic model was determined from laboratory data and adjusted to the geological setting. For this localization neither station corrections nor station weights needed to be applied.

The anisotropic localization provides a physically intuitive result and is therefore the model of our preference. However, residuals for both models, isotropic and anisotropic are of about the same magnitude. Statistically, we can not decide, which model is actually the better one since both lead to a similar quality of the fit. This disappointing conclusion is, however, not at all surprising since the geological situation and the anisotropy at the KTB are rather complex. This complexity is not appropriately reflected by the homogeneous anisotropic model. It should be mentioned that the localizations with the isotropic 3-D heterogeneous model also displayed the lateral shift of a similar size as the localizations with the homogeneous isotropic model. We therefore conclude that anisotropy has a stronger effect on the localization than heterogeneity for the KTB data.

This data case study has demonstrated that the localization of events and the shape of the event cloud are strongly affected if a possible anisotropy of the subsurface is neglected. It would be interesting to repeat our study with a heterogeneous anisotropic model to obtain an improved data fit. This, however, would require a detailed 3-D anisotropic velocity model building which is not possible for the KTB data since seismic borehole observations at only one depth level are available. Also the 3-D reflection seismic data are not suitable since the events in a hard rock environment like the KTB are of diffraction character, i.e., small diffracting/reflecting elements. Such kind of events could not be interpreted in terms of non-hyperbolic moveout owing to the lacking spatial continuity of arrivals.

In contrast to the injection experiment at the KTB we usually have less a priori information on the potential occurrence of events in seismology. We are therefore in a less favorable position than in this study. A systematic shift of the event locations due to an unidentified anisotropy may severely mislead the interpretation of the event distribution. Similar conclusions apply if hydraulic fractures are imaged using the passive seismic method. The orientation, position, and size of the induced fracture may be strongly influenced by an unidentified or ignored anisotropy.

### ACKNOWLEDGMENTS

We are grateful to Svetlana Golovnina and Tina Kaschwich for discussions on the subject and for providing software to set up the anisotropic part of the localization. We thank M. Bonhoff for providing the data including picks and localizations. This work was partially supported by the sponsors of the Wave Inversion Technology consortium, the DGMK (Deutsche Gesellschaft für Erdöl, Erdgas und Kohle) project 593-3, and the German Research Foundation through the ICDP/IODP priority program (Ga 350/14-1).

### REFERENCES

- Baisch, S., M. Bohnhoff, L. Ceranna, Y. Tu, and H.-P. Harjes, 2002, Probing the Crust to 9 km depth: Fluid injections experiments and induced seismicity at the KTB superdeep drilling hole, Germany: *Bulletin of the Seismological Society of America*, **92**, 2369–2380.
- Buske, S., 1999, Three-dimensional pre-stack Kirchhoff migration of deep seismic reflection data: *Geophysical Journal International*, **137**, 234–260.

- Coman, R. and D. Gajewski, 2004, Traveltime computation by wavefront-oriented ray tracing: *Geophysical Prospecting*, **53**, 23–36.
- Ettrich, N. and D. Gajewski, 1996, Wave front construction in smooth media for prestack depth migration: *Pure and Applied Geophysics*, **148**, 481–502.
- , 1998, Traveltime computation by perturbation with FD eikonal solvers in isotropic and weakly anisotropic media: *Geophysics*, **63**, 1066–1078.
- Evans, J., D. Eberhart-Phillips, and C. H. Thurber, 1994, User's manual for simulps12 for imaging vp and vp/vs: A derivative of the "thurber" tomographic inversion simul3 for local earthquakes: USGS Open-File Report 94-431.
- Geiger, L., 1910, Herdbestimmung bei Erdbeben aus den Ankunftszeiten: *K. Ges. Wiss. Gött.*, **4**, 331–349.
- Jahns, E., S. Siegesmund, W. Rabbel, and T. Chlupac, 1994a, Seismic anisotropy: Comparison of lab-, logging and VSP-data: KTB-Report 94-2, 163–168.
- , 1994b, Seismic Anisotropy: Comparison of Lab-, Logging, and VSP-Data: KTB-Report 94-2, A163–A167.
- Kaschwich, T. and D. Gajewski, 2003, Wavefront-oriented ray tracing in 3D anisotropic media: Expanded Abstracts, P-041, 65th EAGE Meeting and Technical Exhibition.
- Leidenfrost, A., N. Ettrich, D. Gajewski, and D. Kosloff, 1999, Comparison of six different methods for calculating traveltimes: *Geophysical Prospecting*, **47**, 269–297.
- Moser, T. J., 1991, Shortest path calculation of seismic rays: *Geophysics*, **56**, 59–67.
- Rabbel, W., 1994, Seismic anisotropy at the Continental Deep Drilling Site (Germany): *Tectonophysics*, **232**, 329–341.
- Rabbel, W., T. Beilecke, T. Bohlen, D. Fischer, A. Frank, J. Hasenclever, G. Borm, J. Kück, K. Bram, G. Druivenga, E. Lüschen, H. Gebrande, J. Pujol, and S. Smithson, 2004, Super-deep vertical seismic profiling at the KTB deep drill hole (Germany): Seismic close-up view of a major thrust zone down to 8.5 km depth: *Journal of Geophysical Research*, **109** (B9).
- Soukina, S., D. Gajewski, and B. Kashtan, 2003, Traveltime computation for 3-D anisotropic media by a finite-difference perturbation method: *Geophysical Prospecting*, **51**, 431–441.
- Thurber, C. and N. Rabinowitz, eds., 2000, Advances in seismic event location, *Modern Approaches in Geophysics*, Lod, Israel. Geophysical Institute of Israel.
- Vanelle, C. and D. Gajewski, 2002, Second-order interpolation of traveltimes: *Geophysical Prospecting*, **50**, 73–83.
- Vidale, J., 1988, Finite-difference calculation of traveltimes: *Bulletin of the Seismological Society of America*, **78**, 2062–2076.
- , 1990, Finite-difference calculation of traveltimes in three dimensions: *Geophysics*, **55**, 521–526.
- Vinje, V., E. Iversen, K. Åstebøl, and H. Gjøystdal, 1996a, Estimation of multivalued arrivals in 3D models using wavefront construction—Part I: *Geophysical Prospecting*, **44**, 819–842.
- , 1996b, Part II: Tracing and interpolation: *Geophysical Prospecting*, **44**, 843–858.
- Waldhauser, F. and W. Ellsworth, 2000, A double-difference earthquake location algorithm: Method and application to the Northern Hayward Fault, California: *Bulletin of the Seismological Society of America*, **90**, 1353–1368.